International Conferences on Recent Advances in Geotechnical Earthquake Engineering and Soil Dynamics

2010 - Fifth International Conference on Recent Advances in Geotechnical Earthquake Engineering and Soil Dynamics

26 May 2010, 4:50 pm - 5:30 pm

General Report — Session 1

Pedro de Alba
University of New Hampshire, Durham, New Hampshire

Kenneth Gavin
University College, Dublin, Ireland

Monica Prezzi
Purdue University, West Lafayette, IN

Theodoros Triantafyllidis
University of Karlsruhe, Germany

Follow this and additional works at: https://scholarsmine.mst.edu/icrageesd

Part of the Geotechnical Engineering Commons

Recommended Citation

DYNAMIC PROPERTIES OF SOILS: LABORATORY AND FIELD METHODS, LARGE-SCALE TESTING

Pedro de Alba
University of New Hampshire, Durham, New Hampshire

Kenneth Gavin
University College, Dublin, Ireland

Monica Prezzi
Purdue University, West Lafayette, Indiana

Theodoros Triantafyllidis
University of Karlsruhe, Karlsruhe, Germany

General Report-Session 1

Introduction

The variety of contributions to this session remind us of the broad range of topics encompassed by geotechnical earthquake engineering and other applications of soil dynamics, and how far we have come since the great 1964 earthquakes of Niigata and Alaska gave such a significant impulse to research in this field. Our report is essentially divided into sections covering innovative laboratory work, field studies for ground response prediction, and foundation behavior under dynamic loads.

We start with a discussion of small-strain laboratory tests involving improved equipment, or new interpretations of results in well-established tests, to determine dynamic soil properties in our classic materials: clean sands and plastic clays. We then discuss similar lab tests on materials such as silty sands, and the testing/modeling of gravels, which, arguably, have received less attention; some very good work has been presented to the conference, but it is obvious that we still have much to find out regarding, for example, the influence of relatively small amounts of fines of different plasticity on sand behavior; or of the effects of grain size distribution and particle strength in gravels.

We then focus on laboratory simulation of the liquefaction behavior of granular soils, and again the difference in undrained behavior of silty sands and silts under monotonic and cyclic loading is a major issue, as is the improved simulation of large-strain behavior after the triggering of liquefaction.

Measurement of shear wave velocity (V_s) is the major concern of our papers regarding case histories of field characterization, with surface-wave measurements predominating, and include attempts to relate field V_s to

penetrometer tests, or to values measured in the lab. A major difficulty which becomes evident when studying this work is the lack of international agreement on how to carry out standard penetration tests, or recover "undisturbed" samples. This certainly deserves the attention of our profession.

Finally, we discuss problems of foundation design; a significant number of our papers refer to large-scale model studies of a range of foundation elements (and methods of site improvement) under controlled conditions. Very interesting work is presented, and gives us significant insight into these problems, but we should recall that the ultimate test of potential design applications resulting from <u>all</u> the research described in this session lies in the observation of full-scale structures under earthquake loading. Ideally, this requires establishing and maintaining very well-characterized and heavily-instrumented field experimentation sites, for which all information would immediately be made accessible to all interested researchers. In many countries, there is great reluctance on the part of funding agencies to support these projects, since they require constant attention, potentially over long periods of time, before they produce significant results. Again this is a goal we should collectively press for.

Dynamic Soil Behavior: Laboratory Measurements

I. Small-Strain Tests: Resonant Column, Bender Elements, DSS tests.

I.(a) Clean Sands and Clays:

A significant number of papers in this session present results from resonant column (RC) tests, either as a basis for design applications or, for example, to compare with values

deduced from shear wave velocity measurements. Others examine the basic assumptions of the test, and propose improvements. Sultaniya et al. (paper 1.14b) have developed a finite element model of the fixed-free device and have simulated tests in torsional, longitudinal and flexural excitation modes. The authors' Figure 5 (below) shows the effects of the length to diameter aspect ratio of the sample on the ratio of the measured values of Young's modulus from flexural or longitudinal excitation, E_{flex}, E_{iso} and shear modulus from torsional excitation G_{iso} to the 'true' shear modulus (G) and elastic modulus (E) values assumed for the isotropic specimen. The conventional 2:1 ratio is shown to have a significant effect on flexural resonance.
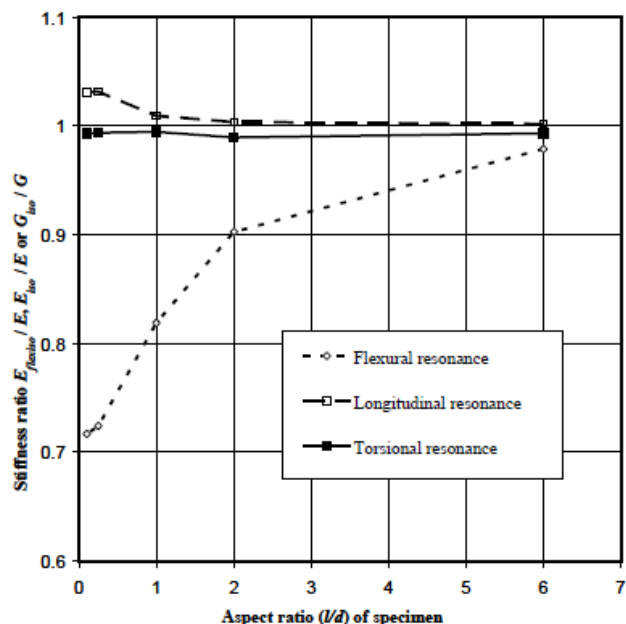

Fig. 5. Ratio of calculated stiffness to the defined stiffness for an isotropic material with slenderness ratio.

The authors remind us, however, that soils are not isotropic; that, as a minimum, we should consider them to be transversely isotropic, and argue that a complete testing program should include tests on specimens carved in both the vertical and horizontal direction. This is definitely not an easy task, and leads to the question of whether there are other ways to measure elastic properties in the horizontal plane.

The use of piezoelectric bender elements and expansion disks to generate S-and P- waves is one possibility, although there are a number of problems involved (proper coupling with the specimen, detection of first arrival, multipath effects, and others). Lo Presti et al. (1.30b) integrate bender elements into the cap and base of a new combined triaxial/resonant column system, and compare modulus values obtained from shear wave velocity, either using the benders as source and receiver, and measuring first arrival, (FA), or first-peak-to-first peak time-of flight, or generating an external signal and finding the time-of-flight (RR)

between receivers. Except for the use of first arrival (FA) to determine velocity, the authors' Figure 3 (opposite) shows good agreement with values from a conventional resonant column test for the vertically-propagating signal; reliable measurement of horizontal values remains an issue.
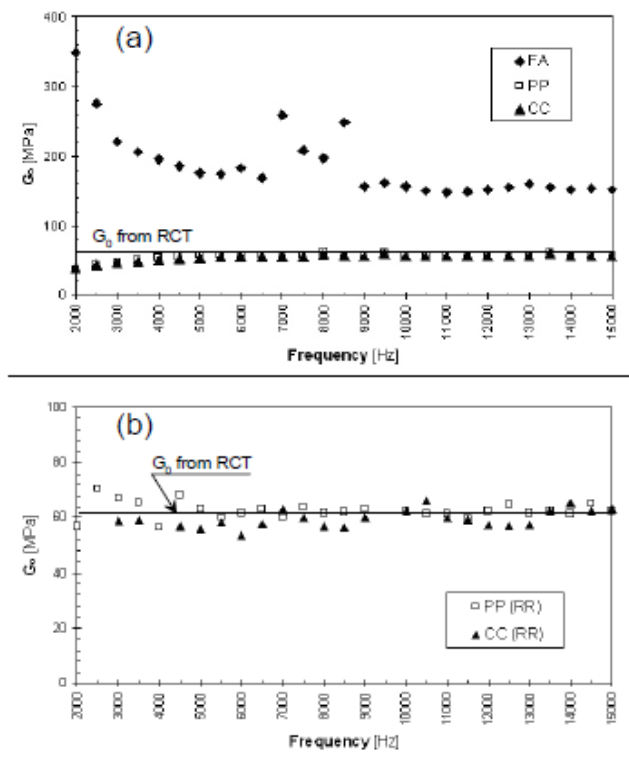

Fig. 3. Measured values of G_0: a) bender elements as source and receiver; b) both bender elements as receiver.

Capar and Ishibashi (1.51a) show results for low-strain measurements in triaxial specimens using bender elements to generate both P and S-waves with frequencies in the 20 kHz range in the vertical direction, and P-waves with similar frequencies in the horizontal direction; in this study, the medium-dense sand specimens were modeled as cross-anisotropic, and a technique to recover the five required elastic parameters from the wave velocity measurements is proposed. Interestingly, the degree of isotropy of the specimens was found to increase with confining pressure, to the extent that the specimens exhibited isotropic behavior at pressures of 200 kPa or more.

We should note from the previous discussion that shear wave measurements with bender elements are carried out at frequencies much higher than the earthquake range; it is commonly accepted that the maximum shear modulus G_{max} in the small-strain elastic-behavior range of soil is frequency-independent. However, Ashlock and Pak (1.31b) present results of an analysis of random vibrations applied to a modified free-free resonant column specimen of silica sand, for which a match of calculated base/cap transfer functions to observed behavior requires postulating a

significant G-gradient in the specimen, and a frequency-dependent damping ratio as shown in the author's Figure 8b (next page).

(b)
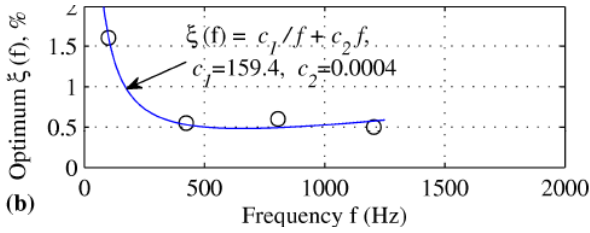
The authors maintain that these higher frequency tests are necessary to cover the possible range of frequencies encountered in different soil dynamics problems; these tests, however, emphasize some of the experimental difficulties arising in resonant column tests at high frequencies: e.g. contact between the specimen and the end plates, and possible dispersion effects due to mean particle size and grain size distribution.

This raises the question of effects of grain structure on stress-wave propagation through soils; in this regard, Bui et al. (1.24a) present a new universal void ratio function for small-strain shear modulus determination through a porous-discontinuous soil model in which void ratio effects $F(e) = (1+e)^{-3}$ are incorporated in an equation of the form:

$$G_{max} = A \, F(e)(\sigma')^{n}$$

Where σ' is the mean effective stress and both (A) and (n) must be adjusted to represent particle characteristics, anisotropy, time effects, etc. The authors' Figure 4 (below) shows a good agreement between experiment and the proposed equation.
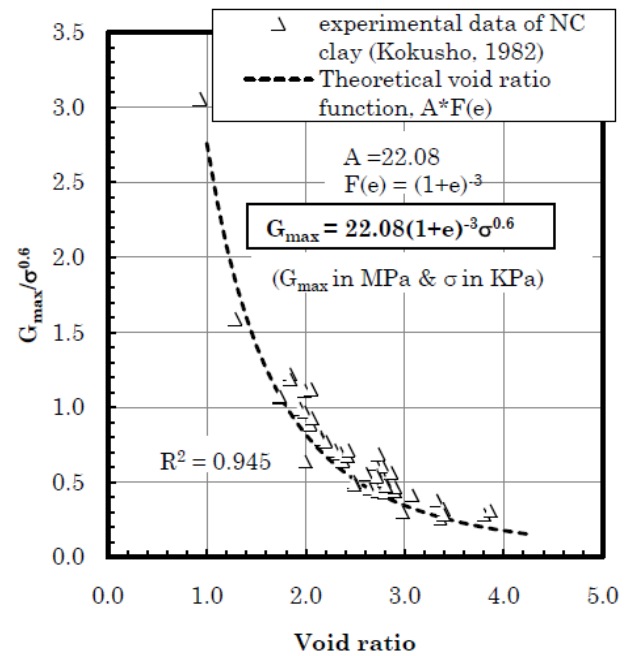

Figure 4: Application of the theoretical void ratio function to G_{max} of soft NC clay measured by Kokusho (1982)

This model assumes that shear wave propagation through the medium is a function of the void ratio, the shear wave velocity through the solid particles and, critically, the propagation velocity through the particle contacts which must be measured experimentally.

Finally, other applications of RC testing and soil properties determination can be found in Park (1.59a), Stavnitser and Nikitaeva (1.12b) and Abuhajar et al. (1.32b).

I.b) Intermediate Soils:

It might be argued that materials which have not received significant attention in small-strain properties testing are silty sands. Wichtmann and Triantafyllidis (1.55a) present results of an extensive series of free-free resonant-column experiments on quartz sands of varying coefficient of uniformity (d_{60}/d_{10}) and fines content, to produce an improved numerical model for predicting maximum small-strain shear modulus (G_{max}) and elastic modulus (M_{max}). The proposed numerical model is a significant refinement of the well-known Hardin-Black model. Notably, their results show that a major factor in determining modulus value is not the mean grain diameter, but the coefficient of uniformity, and that small-strain moduli exhibit a very significant decrease in magnitude for fines content between 0 and 10%, as shown in their Figure 12.   A refinement of the Harding-Drenevich modulus degradation factor is also presented, and shown to also be affected by fines content and coefficient of uniformity, albeit not so dramatically as the small-strain moduli.
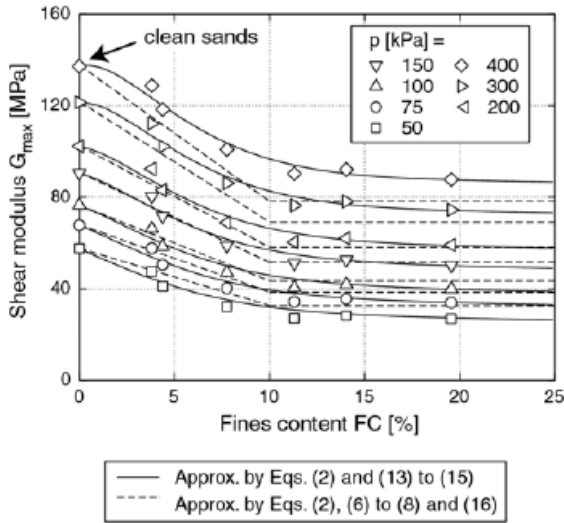
Fig. 12: Decrease of small-strain shear modulus G_{max} with incrasing fines content, data for a constant void ratio e = 0.825

Regarding the limiting strains beyond which modulus degradation takes place, paper (1.15a) by Tabata and Vucetic defines a threshold shear strain, γ_{td} in direct simple shear tests (DSS) for clays, beyond which the original particle contact structure is irreversibly damaged, leading to a decrease in (G). γ_{td} is found to be smaller than the threshold shear strain for volume change, γ_{tv}, and for buildup of residual pore water pressure γ_{tp} ,and depends on PI as shown in the authors' Figure 11 (next page). The reason for his difference in threshold shear strains is not clear, and a physical explanation needs further investigation.
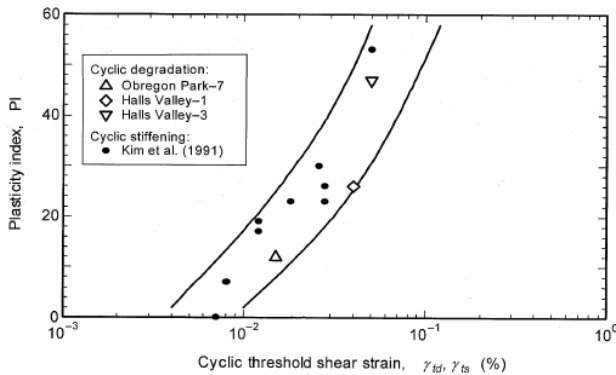

Fig. 11   Trend of γ_{td} for cyclic degradation and γ_{ts} for cyclic stiffening with PI

Settlement of clayey sand under cyclic load is the subject of Vucetic et al.'s contribution (1.14a); DSS tests were carried out on a compacted clayey sand (37% fines, 14% clay, saturation between 80-99%). The threshold shear strain for volume change, γ_{tv} was found to be about 0.02%, below which there was no settlement. As expected, applied vertical stress and void ratio significantly affected the results, but they also note an important effect of degree of saturation, which they attribute to the interaction of pore air with pore water under cyclic load. This effect will require further research, with more sophisticated instrumentation.

As an extreme case of materials other than clean sands and clays, Shariatmadari et al. (1.41a) present results of large triaxial and direct shear tests on municipal solid waste (MSW) material. These results seem to confirm previous findings which show that MSW resistance is sensitive to strain rate, and resistance increases as the strain rate increases.

Finally, it is obvious from the previous discussion that it would be desirable to have a large database of cyclic tests carried out on similar equipment, for comparisons of dynamic behavior of different materials. Matesic et al. (1.07b) describe the development of a computer database for archiving, organizing and comparing data from large numbers of tests using NGI-type DSS and dual DSS devices, thus covering a shear strain range between 0.0003% and 10%. This database permits ready comparisons of the effects of shear strain amplitude, strain rate, and effective confining pressure on soils with different index properties and OCR. Summary results for tests with PI between 0 and 44% confirm, for example, that for all soils tested, the largest variation in normalized shear modulus occurs between about 0.005% and 0.1%, (which, it should be noted, is consistent with the results of Seed and Idriss, 1970, albeit from a much smaller database), the position of the individual curve depending on the PI. Other comparisons show how damping ratio in sands, non-plastic silts, and clays decreases with vertical effective stress, as shown in the authors' Figure 15 which again, is consistent with the curves presented by Seed et al. (1986).
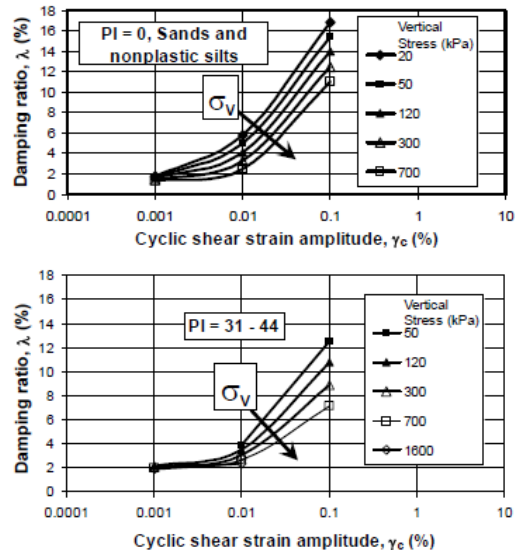

Fig. 15. Effect of vertical stress on the equivalent viscous damping ratio curve for two groups of soils derived from Fig. 13 above (Hsu and Vucetic, 2002)

II. Undrained Behavior of Sands: Liquefaction.

As for small-strain behavior discussed above, the effect of silt on soil response is a topic which deserves more attention in liquefaction studies. Murthy et al. (1.15b) report on results of a series of undrained monotonic triaxial tests carried out to investigate the effects of silt content on the evolution of undrained material behavior as it is loaded to the critical state. Results are presented for specimens with 0, 5%, 10% and 15% silt, consisting of ground silica (SilCoSil), prepared by slurry deposition and moist tamping. As might be expected, increasing silt content causes a shift in the position of the critical state line downwards in an e-log p′(mean effective stress) plot; the effect of sample preparation vanishes with large strains, and the friction angle at the critical state, φ_{cs}, is relatively insensitive to fines content up to 10% ($\varphi_{cs} = 30.2^o$ to 31.8^o) with a clear jump as fines content goes to 15% ($\varphi_{cs} = 34.4^o$). These are interesting conclusions, and emphasize the importance of further research into the effects of other types of fines (different grain size ranges, plasticity), the effects of cyclic vs. monotonic loading on the soil structure, and the imposition of strain levels significantly higher than those attainable in triaxial tests.

In this regard, Monkul and Yamamuro (1.23a) show results of a series of triaxial tests exploring the susceptibility to low-strain temporary liquefaction behavior, under undrained monotonic loading, of a Nevada Sand with 20% silt content, using two different silts. The tests show that the susceptibility to temporary liquefaction is strongly dependent on the gradation of the silt, described through the ratio of D_{50} of the sand to D_{50} of the silt ($D_{50\text{-sand}}/d_{50\text{-fines}}$), with the lower ratio giving the higher susceptibility. The authors speculate that this is because the finer silt (SilCoSil) occupies pore space between the sand particles, allowing more sand-to-sand contacts, whereas the coarser silt presumably fosters a tendency to higher volumetric contraction by forming a larger part of the sand 'skeleton'. They also propose that the different grain angularity of the two silts may play a role. These results are highly suggestive, and, as mentioned above, deserve to be extended to a larger range of silt types and silt contents, as well as the application of cyclic vs. monotonic loads. In a related paper (1.34b), the authors review sample preparation techniques for preparing silty sand specimens, and propose a new 'tubed funnel deposition' method as being closest to preserving the number of metastable contacts, where silt grains separate the sand grains, as found in natural soils.

The undrained behavior of a sandy silt (ML) in triaxial tests under monotonic, and both symmetrical and non-symmetrical cyclic loading, is the subject of Saglam and Bakir's contribution (1.47a). It is interesting to note that, even at 10% axial strain under cyclic load, only one of 26 saturated specimens reached an excess pore pressure ratio of 100%.

Yang and Sze (1.25a) present a thorough analysis of non-symmetrical loading effects on cyclic strength in triaxial tests for clean sand specimens placed at a large range of densities. The paper shows, for example, that a low static shear initially leads to an increase in cyclic resistance with deviatoric stress ratio for loose sand, but that a further increase of deviatoric

stress ratio on this loose material results in a decrease in resistance (authors' Figure 7), and the paper offers an explanation for this behavior.
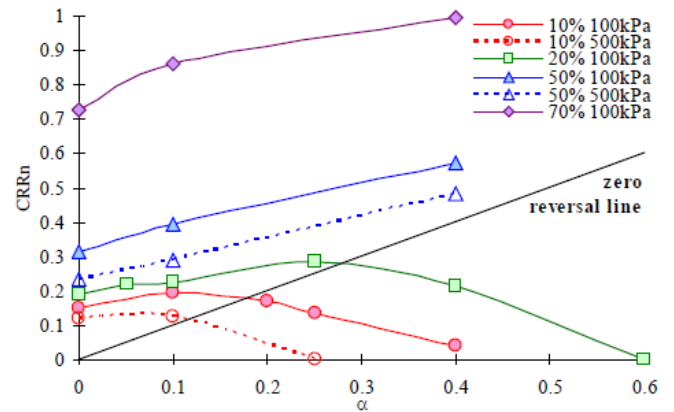

Fig. 7. Cyclic strength of Toyoura sand at different initial states under initial shear impact.

These contributions do raise the question, however, of the effect of triaxial loading systems on liquefaction simulation, and indicate the need for comparison with DSS results, such as those of Boulanger et al. (1991).

With regard to DSS testing for liquefaction behavior, a very interesting comparison of results from strain-controlled constant-volume and constant vertical load liquefaction tests is presented by Jafarzadeh and Sadeghi (1.11a). Specimens of a fine and medium sand were prepared by a moist-tamping procedure at 5% water content to relative densities of approximately 30 and 70%, and tested in a stacked-ring DSS apparatus. Constant vertical load specimens were saturated, constant-volume tests carried out at placement water content. In both cases, shear strain levels of 1% and 1.5% were applied. Basically, results showed that, compared on a cycle-by-cycle basis, the constant-load liquefaction tests started with higher initial shear modulus (G) values, but showed greater change in (G) with number of cycles prior to liquefaction than the constant volume tests and, very importantly, the constant-volume tests showed little change in damping ratio with increasing number of cycles towards simulated liquefaction, or with applied shear strain amplitude, which contrasts significantly with the saturated undrained tests. This study raises some very interesting questions regarding the applicability of constant-volume tests to study the undrained behavior of granular soils, and merits consideration in the interpretation of tests by Haeri and Pouragha (1.08b) regarding the effect of static shear on liquefaction behavior.

The application of large strain levels, modeling liquefied sand behavior beyond the 'triggering' of liquefaction is not possible in conventional triaxial or DSS devices. In this regard, the ring shear device is the best tool for simulating large-strain behavior in the laboratory. Sandoval et al. (1.05b) applied this technique to study the large-strain behavior, and strain- rate effects, on liquefied residual strength of a clean fine sand.

Results from strain-controlled tests showed that liquefied sand behaved as a 'stress thinning' fluid, best modeled using the Herschel-Bulkley equation. Results are compared to another, smaller-scale, stress-controlled test, in which a square metal coupon is pulled through a liquefied triaxial specimen by a dead weight, and, approximately, to large-strain residual strength values back-calculated from field failures as shown in the authors' Figure 13 (next page). Laboratory results were found to follow the same trend as the field data, with the ring-shear results (green) forming an upper bound to the field data and the coupon tests (red triangles, blue squares), a lower bound.

III. Other Laboratory Techniques: Instrumentation.

Two papers have been presented on this topic, both regarding new instrumentation for centrifuge testing; Coe and Brandenberg (1.21b) show a novel application of an ultrasonic P-wave reflection imaging system which can be used to define complex layering, identify buried anomalies and provide incremental visualization of the effects of complex loading histories in geotechnical models

Li (1.23b) describes a new method for measuring the spatial variability of strains in soils. The method is based on electrical resistivity concepts, establishing electromagnetic fields in a saturated soil. A mesh of electrodes within the soil is placed and low frequency alternating currents are injected via the electrodes. The displacement of the soil is related to the change of electrical potential measured on the electrode located at that point. From the potential distribution based on
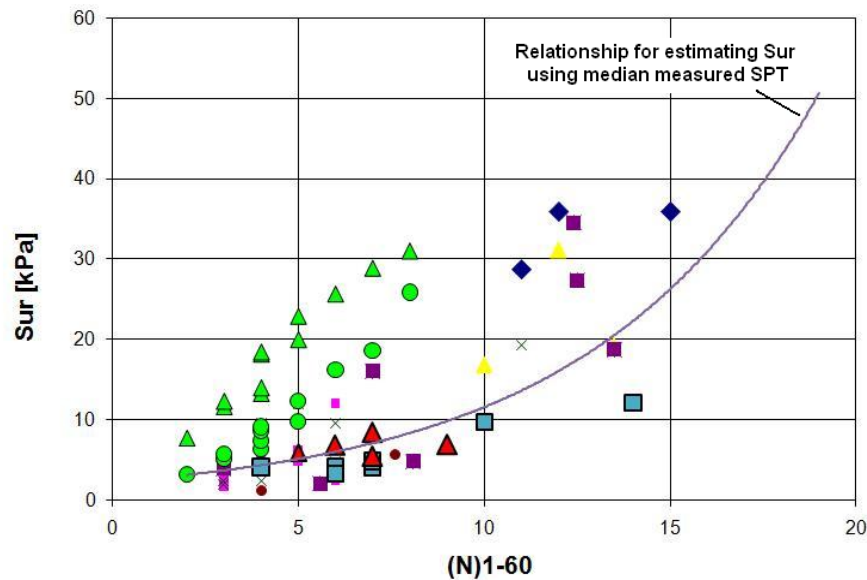

Fig 13. Comparison of field Sur-values from Idriss and Boulanger (2007) with triaxial coupon and ring shear values

.

electrical concepts with closed form solutions using Green's function, the displacement is calculated. From the displacement of the mesh points the strains can be calculated using basic mechanical/geometrical concepts. The method is promising, but further development is required; one important issue is the choice of the material of the electrode whose density and stiffness should be close to that of the surrounding soil medium. The method has been tested in centrifuge experiments which show that the estimated vertical deformations are acceptable, but that horizontal deformations do not match as well.

Dynamic Soil Behavior: Soil Models

Three contributions to this session propose new soil models, two for clays and, going to the other extreme, one for gravels. Stamatopoulos (1.03a) proposes an improved model for predicting large-strain clay behavior along failure surfaces. The use of the constant-volume ring shear test is advocated as the only experimental device for determining clay behavior at large strains. The analytical model involves 10 parameters for undrained behavior, 8 of which can be determined in conventional direct simple shear or direct shear tests, and 2 which must be found from constant-volume ring shear tests. The model is successfully compared to available published ring-shear data, as shown in the author's Figure 5 (opposite), although further verification against additional data sets would be desirable.

Taiebat and Kaynia (1.09a) apply a modified version of the SANICLAY model to clay slope analysis. This model accounts for soil anisotropy by introducing user-defined parameters to rotate the yield and plastic potential surfaces. The importance of anisotropy is demonstrated , wherein the horizontal displacement experienced by an example slope increased by 30% when anisotropic hardening was included in the model.
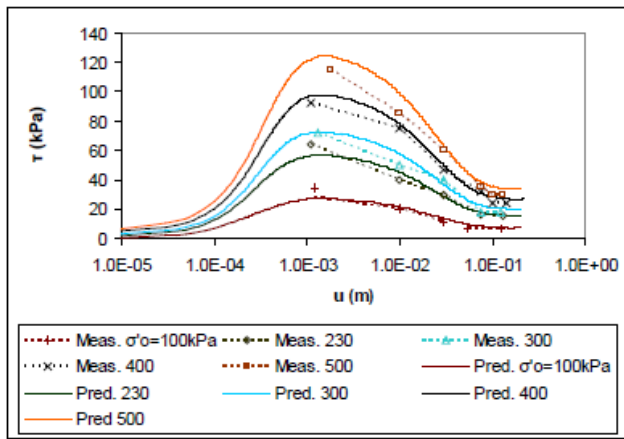
Figure5. Measured and predicted response constant-volume ring shear tests, Bootlegger Cove clay

Finally, Modoni and Gazzellone (1.28a) describe a new model for compacted gravels , which requires 16 experimentally-determined parameters. The application of the model is illustrated by results obtained from a crushed sandstone material. Calculated values of normalized shear modulus (G/G_{max}) and of damping are compared with those obtained in cyclic triaxial tests by Seed et al. (1986); normalized G/G_{max}-values follow the same trend, but plot above the upper boundary of the Seed et al. curves, and are seen to be sensitive to confining stress, whereas damping curves plot approximately at the lower bound of the Seed et al. curves. There seems to be very little influence of void ratio in the e = 0.2 - 0.5 range, whereas Seed et al. show a significant effect of relative density, and thus void ratio, on G-values at shear strain levels below 0.01% for a crushed sandstone gravel . Application of this model is illustrated through finite difference analyses of a 15-m thick deposit of gravel; interestingly, for $0.1 \leq e \leq 0.5$, amplification is seen to be the same up to a base acceleration of 0.3g, above which the loosest material is seen to have the highest amplification.

Dynamic Soil Behavior: Field Measurements

Contributions to this conference on characterization of natural soil deposits for earthquake-response prediction concentrate predominantly on application of surface wave techniques for obtaining shear wave velocity and, if possible, comparison of these measurements with laboratory tests on 'undistarbed' samples, or with other field tests, notably the standard penetration test (SPT). In this regard, one issue which arises from a review of these papers is the urgent need for international agreement on how SPT tests are to be conducted and documented, and how SPT values are to be normalized. It is imperative that, in any contribution to the geotechnical literature, there should be a clear statement by researchers on how this was done in their particular study. A similar issue arises with regard to 'undisturbed' samples; in some parts of the world, for example, a thin-walled tube driven by a drill hammer is considered to produce an undisturbed sample, whereas in other parts this would be unacceptable. Again, a clear description of how samples are obtained is essential.

Table 1 (below) summarizes the studies of various researchers noting proposed correlations between different intrusive and non-intrusive tests to determine Vs.

Particular applications of measured Vs values include a study of the liquefaction potential of a 200,000 year old sand deposit by Geiger et al. (1.34a). Shear wave velocities from seismic cone penetration tests in a surface deposit of fine beach sand were found to be about 47% higher than would be expected for a young, 10-yr-old sand deposit, reflecting the effect of deposit age, and thus increased liquefaction resistance.

Another application, proposed by Yi (1.57a), is a direct correlation of shear wave velocity to magnitude of lateral spreading in liquefied sand deposits. The author applies the technique to an observed lateral spread at Moss Landing, California during the 1989 Loma Prieta earthquake and compares it with other penetrometer-based techniques, reporting good agreement, although local calibration of the method seems desirable.

TABLE 1
Field Measurements

Paper Number	First Author	Soil types	Primary Vs-measurement technique	Comparison with other methods
1.31a	A. Cavallaro	Stiff-fissured desiccated clays	Marchetti seismic dilatometer (SDMT)	Noise analysis of surface waves (NASW), downhole
1.02b	K. Aykin	Various	Seismic cone (SCPT)	SDMT, SPT

1.28b	S. Lazcano	Pumice	Refraction microtremor (ReMi)	Not possible
1.20a	E. Leung	Weathered rock	Various surface and downhole, crosshole	SPT
1.29b	Z. Chik	Residual	MASW[1]	SPT
1.13b	P. Anbazhagan	Various	MASW	SPT
1.01b	N. Satyam	Various	MASW	
1.36a	S. Ghose	Interbedded clays and silts	Downhole	SPT
1.21a	M. Akin	Clays and sands	SPT-based Uphole	SPT

(1) MASW = Multichannel Analysis of Surface Waves

Liquefaction/cyclic failure of fine-grained soils is the focus of Bilsel et al. (1.58a); they give an lucid overview and discussion of possible methods of predicting failure potential of these soils as applied to a highly-vulnerable area of Cyprus.

Finally, concerning possible improvements to our Vs-measurement techniques, only one paper is presented; Areias (1.20b) discusses problems with the widely-used down-hole pseudo-interval method, and a test configuration that will result in a reduced variability of measurements.

Dynamic Behavior of Foundations

Sixteen papers were submitted to this session on various aspects of foundation design, each discussing separate aspects of foundation behavior under dynamic loads, or presenting case histories of site exploration. Given the lack of an overarching theme, the reporters decided it would be most effective to tabulate the papers (Table 2, pp. 9-10) with brief remarks regarding what they considered to be the salient results.

Ground Improvement – New Techniques

An original way of reducing liquefaction potential in sands by continuous injection of microbubbles is proposed by Nagao et al. (1.26b). A large scale (5 m high, 10 m long and 3.6 m wide) model was constructed on a shaking table. Silica sand used was placed at an average relative density of 46%, giving SPT values in the 7 to 13 BPF range. The effectiveness of reducing the degree of saturation, S_r, from 100% (Case B) to 95% (Case A) is illustrated in the authors' Figure 22, which shows the accumulated shear strain ($\Sigma\gamma$) against the excess pore pressure ratio generated during two acceleration events (100 Gal and 150 Gal). It is clear that while the untreated ground essentially liquefied during these loading events, the treated ground (Case A) developed insignificant excess pore pressures and relatively small deformations.
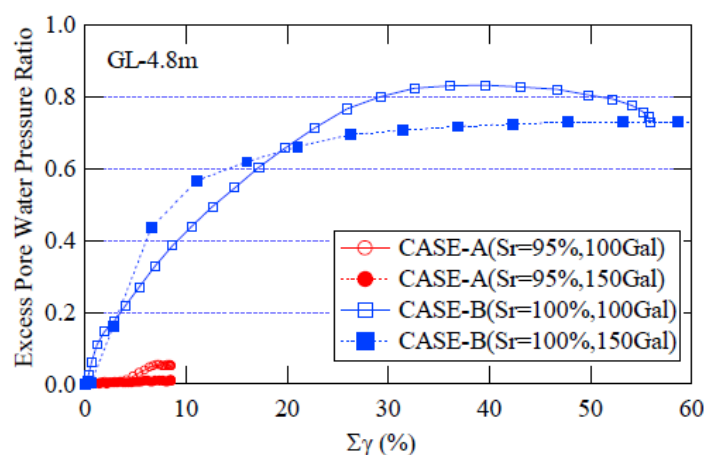

Fig.22 Relationship between excess pwp ratio and $\Sigma\gamma_{MAX}$

scale model tests is reported by Saran et al. (1.18a) The authors note that while many studies have considered the response of reinforced soils when subjected to static loading, the majority of studies of cyclic loading have been performed in small-scale, i.e., cyclic triaxial tests. The authors' experiments were performed using a 600 mm-high test sample placed on a shaking table. The effectiveness of providing 3 to 5 layers of geogrid reinforcement in a sand model of very low relative density (25%) was tested.

The applied horizontal acceleration varied from 0.1g to 0.4g and the frequency was constant at 5Hz. The results show that while samples with no geogrid liquefied in all cases, the provision of geogrids reduced the excess pore pressure ratio by between 10% for an acceleration of 0.4g, to 30%, for an acceleration of 0.1g, and prevented liquefaction.

Finally, Yang and Salvati (1.05a) show the effects of adding cement on small-strain properties of three sands, placed at relative densities of 60%-95%. Two different types of cement (type III Portland cement and gypsum) were considered, with cement contents ranging from 2.5% to 7.5% by weight. The

authors' Figure 5 shows results of bender element tests to find small-strain shear modulus (G_{max}); as might be expected, the higher Portland cement contents showed the largest increases in G_{max} but also showed the greatest nonlinearity of the shear modulus degradation and damping curves in resonant column tests.
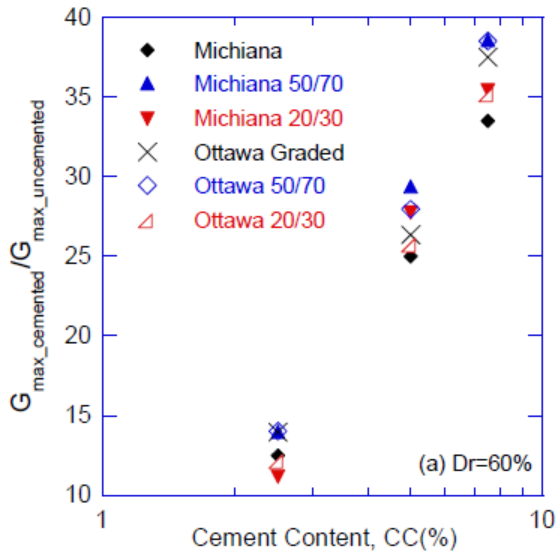
Table 2
Dynamic Behavior of Foundations

Paper	First Author	Remarks
1.24b	P. Wilson	Large-scale experiments were conducted to measure passive pressures behind a simulated bridge abutment with a well-graded sand backfill. A finite element (FE) simulation was carried out and checked against experimental results. The FE technique then permitted extension of the results to investigate the effects of different backfills and wall heights. Non-linear hyperbolic spring models are provided for 32 combinations of backfill soils and wall heights, for use in pushover analyses and dynamic simulations.
1.09b	W.-J. Chang	Presents results of a large-scale model test of a two-pile wharf section, rigidly connected to a deck, with piles extending through a liquefiable slope. Measurements showed very significant screening by the lead pile, and the importance of considering the effect of excess pore pressure on the p-y curves is emphasized.
1.17b	V. Whenham	A review of methods to analyze vibro-drivability of piles and sheetpiles is presented; results from three databases of field results are compared with current analysis methods, and improvements are recommended.
1.11b	J. Moreno Robles	Describes a facility for full-scale testing of railway track structures of high-speed trains. Tests simulate passage of 2.4 million axles at speeds of 300-360 km/hr. Variation of the downward 'ratcheting' of the track ballast with accumulating load repetitions and increasing speed is described.
1.29a	N. Sako	Large-scale model foundation blocks were isolated by different combinations of industrial wastes combined with an asphalt binder, placed in a trench around the block. Peak accelerations were reduced by approximately 30% compared to an un-isolated block.

1.35a	K. Kim	An improved formula is proposed for estimating peak particle velocities from free-falling masses, e.g. during large structure demolition or deep dynamic compaction.
1.38a	H. N. Ramesh	An investigation of the variation of resonant frequency of footings of width (B) on medium-dense sand, with distance (H) above a rigid base. For both saturated and dry sands, resonant frequency was seen to decrease with the ratio H/B, with little difference for H/B>2.
1.54a	V. A. Barvashov	A design method for soil-nail reinforced slopes in c-φ soils is described. Nail resistance is not modeled as a series of point loads, but as a stress along the potential failure surface, the 'cohesion deficit;' a pseudo-static analysis is applied, and nails are designed based on the resulting stresses.
1.19b	N. Denies	To better understand vibro-driving processes, laboratory tests were carried out with a sphere-tipped vibrator in dry fine uniform sand. Three distinct behaviors, densification, surface instability and vibro-fluidization were observed, depending on the acceleration level of the probe; e. g. fluidization occurred at probe accelerations > 1.75g.
1.18b	J. L. Maier	Full-scale field tests to study the efficacy of lateral restraint devices (LRD) applied to helical piles. Unfortunately, no comparison data is provided on lateral resistance of similar piles without LRDs.
1.16b	P. Hu	Centrifuge tests simulate normal-fault movement of a layered sand and silt soil profile with a pre-existing fracture, dipping 70°. The zone of surface cracking was found to be reduced, compared to a model without a pre-existing fracture, and strains were not observed to concentrate in a localized shear band.
1.06b	L. Bozo	An example of a very thorough site exploration program for a major industrial site.
1.33a	B. N. Madhusudhan	Presents dynamic properties of natural and synthetic rubber specimens for application to machine/foundation isolation.
1.06a	J. Najihamodi	Gives an example of interferometer synthetic aperture radar (InSAR) as a tool to plot large-scale ground subsidence; accuracy of $\pm$ 2 cm is reported
1.27b	R. Moss	Basically a description of the test set-up-procedure of a 2.3 m-diam. flexible-wall barrel platform for a proposed shaking table experiment on model underground structures in a clay deposit.
1.33b	J. Steidl	A description of the two heavily-instrumented earthquake geotechnical test sites in southern California: Garner Valley and Wildlife liquefaction site.
1.49a	R. P. Sharma	Provides an overview of currently-employed ground improvement methods.

References.

Boulanger, R. W., R. B. Seed, C. K.Chan, H.B. Seed and J. B. Sousa [1991]. *"Liquefaction Behavior of Saturated Sands under Uni-Directional and Bi-Directional Monotonic and Cyclic Simple Shear Loading."* Geotechnical Engineering Report No. UCB/GT/91-08, University of California, Berkeley.

Seed, H. B. and I. M. Idriss [1970]. *"Soil Moduli and Damping Factors for Dynamic Response Analyses."* Report EERC 70-10 Earthquake Engineering Research Center, University of California, Berkeley.

Seed, H. B., R. T. Wong, I. M. Idriss and K. Tokimatsu [1986]. *"Moduli and Damping Factors for Dynamic Analyses of Cohesionless Soils."* Journal of Geotechnical Engineering, ASCE, Vol. 112, No. 11, pp. 1016-1032.